

Nonlocality in complex networks

Chengwei Wang,¹ Celso Grebogi,¹ and Murilo S. Baptista¹

¹*Institute for Complex Systems and Mathematical Biology,
University of Aberdeen, King's College, AB24 3UE Aberdeen, United Kingdom.*

(Dated: May 3, 2019)

Understanding the interactions among nodes in complex networks are of great importance, since it shows how these nodes are cooperatively supporting the functioning of the systems. Scientists have developed numerous methods and approaches to uncover the underlying physical connectivity based on measurements of functional quantities of the nodes states. However, little is known about how this local connectivity impacts on the non-local interactions and exchanges of physical flows between arbitrary nodes. In this paper, we show how to determine the non-local interchange of physical flows between any pair of nodes in a complex network, even if they are not physically connected by an edge. We show that such non-local interactions can happen in a steady or dynamic state of either a linear or non-linear network. Our approach can be used to conservative flow networks and, under certain conditions, to bidirectional flow networks .

PACS numbers: 89.75.Fb, 05.45.Xt

Research on complex networks has been attracting the attention of many scientists for several decades [1–13]. If the topology of physical connections between any nodes in a complex network is known (such as in a power grid), one wishes to understand how this topology of the connected nodes drives large-scale non-local behaviour of the network [14–16]. To understand large-scale behaviour of complex networks, it is imperative to develop an approach capable of calculating how much physical flow goes from one node to another one through all possible existing paths, a quantity that we refer in this work as “hidden” flow, since this quantity is usually inaccessible from measurements and it is unknown.

In this paper, we introduce the flow tracing method which is known in electrical engineering to track power flows [17–26]. This method applied to power grids not only provides the information of how much power is supplied by a particular generator to a particular consumer, but also helps energy companies to cost proper revenue to energy suppliers and to charge proper wheeling fee from consumers. We avail from this approach to demonstrate how to calculate the hidden flow between any two nodes in conservative flow networks [27], by only requiring information about the adjacent flows between any two connected nodes. This work thus provides a rigorous way to gauge the non-local interactions among nodes in a network. The applicability of the method is enormous since flow networks can be used to model many complex networks, such as transportation networks, water networks, gas and oil networks and power grids. Furthermore, we extend the method to provide an instantaneous picture of how nodes interact non-locally in non-linear networks by constructing linear equivalent model to these networks. We also discuss the application of the method to bidirectional networks, such as transportation networks.

A flow network is a digraph, $\mathcal{G}(\mathcal{V}, \mathcal{E})$, where \mathcal{V} and \mathcal{E} are the sets of nodes and edges, respectively. The direction of an arbitrary edge in \mathcal{G} corresponds to the direction of the physical flow on it. A flow network normally contains

three types of nodes: (i) the source node [e.g., node 1 or 2 in Fig. 1 (a)], which has a source injecting flow into the network; (ii) the sink node [e.g., node 3 or 4 in Fig. 1 (a)], which has a sink taking flow away from the network; (iii) the junction node [e.g., node 5 in Fig. 1 (a)], which distributes the flow. We define f_{ij} to be the *adjacent flow*, or simply the *flow*, between nodes i and j , which is the measurable flow coming from nodes i to j through edge $\{i, j\} \in \mathcal{E}$. Particularly, $f_{ij} = 0$ if node i is not physically connected with node j . In this paper, we consider the conservative flow networks, which satisfy the following properties: (i) the adjacent flow from node i to node j is the opposite of that from node j to node i , i.e., $f_{ij} = -f_{ji}$; (ii) the adjacent flow is conserved at a junction node, i.e., $\sum_{j \in \mathcal{V}} f_{ij} = 0$, where node i is a junction node; (iii) there is no loop flow representing a closed path in a flow network, where a loop flow is shown in Fig. 1 (b); (iv) there is no isolated node in the network, i.e., every node must be connected to at least one other node in the network. A path in a digraph \mathcal{G} from node i to node j , $P(i, j) = i \{i, i'\} i' \{i', i''\} \cdots \{j', j\} j$, is an alternating sequence of distinct nodes and edges starting from node i and ending at node j , in which the directions of all edges must coincide with their original directions in \mathcal{G} . The *hidden flow*, $f_{i \rightarrow j}$, is defined to be the summation of the flows starting from node i and arriving at node j through all possible paths from node i to j .

Normally, we can measure or calculate the adjacent flows in a flow network, but it is not easy to obtain the hidden flows, a quantity typically not accessible through measurements. We find the calculation of hidden flows based on the information of adjacent flows, in a conservative flow network, by the “flow tracing” method.

Define the *node-net exchanging flow* at node i by

$$f_i = \sum_{j=1}^N f_{ij}. \quad (1)$$

If node i is a source node, we have $f_i > 0$; we denote

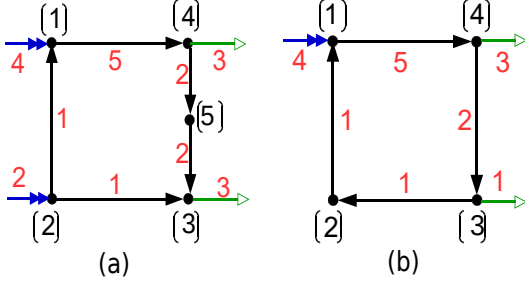


FIG. 1. (colour online) (a) A flow network without loop flow. (b) A flow network with loop flow. The black numbers in square brackets are labels of nodes, the red numbers are adjacent flows, the blue lines with double filled arrows are flow sources, the green lines with unfilled arrows are flow sinks, and the black lines with single filled arrows are directed adjacent flows between nodes.

f_i by f_i^s as the amount of the *source flow* being injected into the network from a source at node i . We set $f_i^s = 0$ if node i is a sink node or a junction node. If node i is a sink node we have $f_i < 0$; we denote $f_i^t = -f_i > 0$ to indicate the amount of the *sink flow* leaving the network from the sink at node i . We set $f_i^t = 0$ if node i is a source node or a junction node.

Assume there is a positive flow from node i to node j , denoted by $f_{ij} > 0$. We use f_{ij}^{out} to indicate f_{ij} as an *outflow* from node i arriving at node j , and f_{ij}^{in} to represent f_{ij} as an *inflow* at node j coming from node i . Thus, $f_{ij} = f_{ij}^{out} = f_{ij}^{in} > 0$. f_{ij} can be positive, negative or zero in a flow network. However, we restrict any outflow or inflow at a node to be a non-negative number. This means that, if $f_{ij} < 0$, we force f_{ij}^{out} and f_{ij}^{in} to be zeros. Analogously, $f_{ij} < 0$ means $f_{ji} > 0$, we have $f_{ji}^{out} > 0$ to denote the outflow from node j to node i and $f_{ji}^{in} > 0$ to be the inflow at node i from node j .

Define the *total inflow* at node i by

$$f_i^{in} = f_i^s + \sum_{f_{ji} > 0} f_{ji} = f_i^s + \sum_{j=1}^N f_{ji}^{in}, \quad (2)$$

and the *total outflow* at node i by

$$f_i^{out} = f_i^t + \sum_{f_{ij} > 0} f_{ij} = f_i^t + \sum_{j=1}^N f_{ij}^{out}. \quad (3)$$

In a conservative flow network, the total inflow of a node is equal to its total outflow, i.e., $f_i^{out} = f_i^{in}$. We assume $f_i^{out} = f_i^{in} > 0, \forall i$, meaning that each node in a flow network must exchange flow with other nodes, i.e., no node is isolated.

The *proportional sharing principle (PSP)* [22, 28] states that for an arbitrary node, a , with m inflows and n outflows (Fig. 2) in a conservative flow network, (i) the outflow on each outflow edge is proportionally fed by all inflows, and (ii) by assuming that node i injects a flow f_{ia}^{in} to node a , and node j takes a flow f_{aj}^{out} out of node a

, we have that the *node-to-node hidden flow* from node i to node j via node a is calculated by

$$f_{i \rightarrow j} = f_{ia}^{in} \frac{f_{aj}^{out}}{f_a^{out}}, \quad (4)$$

or by

$$f_{i \rightarrow j} = f_{aj}^{out} \frac{f_{ia}^{in}}{f_a^{in}}. \quad (5)$$

Equations (4) and (5) result in the same value of $f_{i \rightarrow j}$, since $f_a^{out} = f_a^{in}$. Equation (4) represents the *downstream flow tracing* method, where we start tracing the hidden flow from a source node i to a sink node j , by using the percentage, f_{aj}^{out}/f_a^{out} , to indicate the percentage of f_{ia}^{in} that goes to j . Equation (5) denotes the *upstream flow tracing* method, where we trace the flow from a sink node j to a source node i , by knowing the proportion of f_{aj}^{out} is provided by f_{ia}^{in} . We just deal with the downstream flow tracing in the main context of this paper and explain the upstream flow tracing by an example in the supplementary material [29].

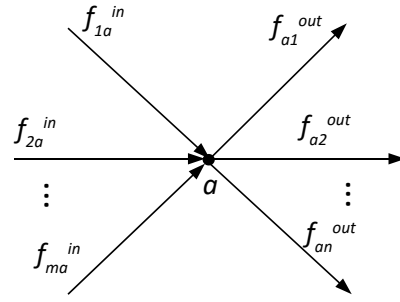


FIG. 2. A node a with m inflows and n outflows.

Define the *downstream coefficient* at node a for the outflow f_{aj}^{out} by

$$\kappa_{aj}^d = \frac{f_{aj}^{out}}{f_a^{out}}, \quad (6)$$

to indicate the proportion of the outflow at edge $\{a, j\}$ to the total outflow at node a . Define the *upstream coefficient* at node a for the inflow f_{ia}^{in} by

$$\kappa_{ai}^u = \frac{f_{ia}^{in}}{f_a^{in}}, \quad (7)$$

denoting the proportion of the inflow at edge $\{i, a\}$ to the total inflow at node a . Then the calculation of $f_{i \rightarrow j}$ can be simply expressed by $f_{i \rightarrow j} = f_{ia}^{in} \kappa_{aj}^d$ or $f_{i \rightarrow j} = f_{aj}^{out} \kappa_{ai}^u$.

Define the *sink proportion* and *source proportion* at node a by

$$\iota_a^t = \frac{f_a^t}{f_a^{out}} \text{ and } \iota_a^s = \frac{f_a^s}{f_a^{in}}, \quad (8)$$

respectively, where the sink proportion, ι_a^t , indicates the proportion of the sink flow to the total outflow at node a ,

and the source proportion, ι_a^s , indicates the proportion of the source flow to the total inflow at node a . By defining the sink proportion and source proportion, we are now able to calculate the source-to-sink hidden flow from a source at node i to a sink at node j denoted by $f_{si \rightarrow tj}$. From Eq. (2), we know that f_i^s is a part of f_i^{in} , where f_i^s is the source flow at node i . From Eq. (8), we know the proportion of f_i^s to f_i^{in} . According to the PSP, we can then calculate the source-to-sink hidden flow by $f_{si \rightarrow tj} = \frac{f_i^s}{f_i^{in}} f_{i \rightarrow j} \frac{f_j^t}{f_j^{out}} = \iota_i^s f_{i \rightarrow j} \iota_j^t$. The source-to-sink hidden flow is different from the node-to-node hidden flow between two nodes. For example, in Fig. 1 (a), $f_{s1 \rightarrow t4}$ indicates how much hidden flow from the 4-unit source at node 1 to the 3-unit sink at node 4, which is different from $f_{1 \rightarrow 4}$ that indicating how much hidden flow goes from node 1 to node 4.

In the supplementary material [29], we demonstrate how to use the downstream flow tracing method to trace hidden current flows in a DC network. However, the downstream flow tracing is most suitable for small networks, because finding all the paths with different lengths between any pair of nodes is a huge amount of work in large sized networks. The extended incidence matrix, proposed in Refs. [23–25], solves this problem.

The *downstream extended incidence matrix*, \mathbf{K} , in a flow network including N nodes is an $N \times N$ dimensional matrix, defined by

$$K_{ij} = \begin{cases} -f_{ji}^{in}/f_j^{out} & \text{if } i \neq j, \text{ and } f_{ji} > 0, \\ 1 & \text{if } i = j, \\ 0 & \text{else.} \end{cases} \quad (9)$$

Transform Eq (2) to $f_i^{in} - \sum_{j=1}^N f_{ji}^{in}/f_j^{out} \cdot f_j^{out} = f_i^s$. Considering $f_i^{in} = f_i^{out}$, we have

$$f_i^{out} - \sum_{j=1}^N f_{ji}^{in}/f_j^{out} \cdot f_j^{out} = f_i^s. \quad (10)$$

From Eqs. (9) and (10), we have

$$\mathbf{K}\mathbf{F}^{out} = \mathbf{F}^s, \quad (11)$$

where $\mathbf{F}^{out} = [f_1^{out}, f_2^{out}, \dots, f_N^{out}]^T$, and $\mathbf{F}^s = [f_1^s, f_2^s, \dots, f_N^s]^T$. \mathbf{K} is an invertible matrix [23, 25, 26], thus, $\mathbf{F}^{out} = \mathbf{K}^{-1}\mathbf{F}^s$, implying that,

$$f_i^{out} = \sum_{j=1}^N [\mathbf{K}^{-1}]_{ij} f_j^s, \quad (12)$$

where $[\mathbf{K}^{-1}]_{ij}$ is an entry (i^{th} row, j^{th} column) of the matrix \mathbf{K}^{-1} . Equation (12) indicates that the outflow of node i , f_i^{out} , is fed by every source f_j^s .

Let $\mathbf{C} = \mathbf{K}^{-1}$ be the *downstream contribution matrix*. Considering $\iota_j^s = f_j^s/f_j^{in}$, we have

$$f_i^{out} = \sum_{j=1}^N C_{ij} f_j^{in} \iota_j^s. \quad (13)$$

For a source node j with $\iota_j^s \neq 0$, $C_{ij} f_j^{in}$ indicates the node-to-node hidden flow from node j to node i , i.e., $f_{j \rightarrow i} = C_{ij} f_j^{in}$.

To demonstrate that the hidden flow can be calculated similarly regardless of the nature of the nodes, we introduce an *equivalence principle* and treat any sink or junction node as a hypothetical source node, without altering the original network topology and flows according to what is explained next. If node j is a sink node or junction node with a total inflow $f_j^{in} > 0$ and $\iota_j^s = 0$, we treat node j as a hypothetical source node with $f_j^s = f_j^{in} > 0$, where the hypothetical source takes the place of all the edges injecting flows into j . By this treatment, we have not changed the flows in the network, but we can hypothetically treat node j as a source node with $\iota_j^s = f_j^s/f_j^{in} = 1$, such that the node-to-node hidden flow from node j to node i can also be calculated by $f_{j \rightarrow i} = C_{ij} f_j^{in}$. From our analysis, $C_{ij} = [\mathbf{K}^{-1}]_{ij}$ is a *downstream contribution factor* indicating how much hidden flow goes from node j to i , i.e., $f_{j \rightarrow i} = C_{ij} f_j^{in}$ for any pair of nodes. Then, $f_{sj \rightarrow ti} = \iota_i^s \cdot C_{ij} f_j^{in} \cdot \iota_j^s$ indicates the source-to-sink hidden flow from node j to node i . An example is given in the supplementary material [29] explaining how to apply the downstream extended incidence matrix to carry out flow tracing.

We now formally conclude and extend our work to analyse the nonlocality study in complex networks. Let i, j, m, n, p, q be different nodes in a conservative flow network, where node i has a source, node j has a sink, nodes m, n are connected by edge $\{m, n\}$ with an adjacent flow $f_{mn} > 0$, and nodes p, q are connected by edge $\{p, q\}$ with an adjacent flow $f_{pq} > 0$. The non-local interaction calculation includes the following parts: (i) the node-to-node hidden flow from node i to node j , $f_{i \rightarrow j}$, is calculated by $f_{i \rightarrow j} = C_{ij} f_i^{in}$; (ii) the source-to-sink hidden flow from node i to node j , $f_{si \rightarrow tj}$, is calculated by $f_{si \rightarrow tj} = \iota_i^s f_{i \rightarrow j} \iota_j^t$; (iii) the node-to-edge hidden flow from node i to edge $\{m, n\}$, $f_{i \rightarrow \{m, n\}}$, is calculated by $f_{i \rightarrow \{m, n\}} = f_{i \rightarrow m} \cdot \kappa_{mn}^d$; (iv) the edge-to-node hidden flow from edge $\{m, n\}$ to node j , $f_{\{m, n\} \rightarrow j}$, is calculated by $f_{\{m, n\} \rightarrow j} = \kappa_{nm}^u \cdot f_{n \rightarrow j}$; and (v) the edge-to-edge hidden flow from edge $\{p, q\}$ to edge $\{m, n\}$, $f_{\{p, q\} \rightarrow \{m, n\}}$, is calculated by $f_{\{p, q\} \rightarrow \{m, n\}} = \kappa_{qp}^u \cdot f_{q \rightarrow m} \cdot \kappa_{mn}^d$.

Next, we extend these concepts to show how nodes interact non-locally in non-linear systems by constructing linear model analogous to the non-linear networks. Let the equation

$$\dot{x}_i = S(x_i) - \sum_{j=1}^N L_{ij} \cdot H(x_i, x_j) \quad (14)$$

indicate a dynamic scheme describing the behaviour of N coupled nodes, where x_i is the dynamical variable of each node, $S(x_i)$ is the isolated dynamic function, L_{ij} is the element of the Laplacian matrix, and $H(x_i, x_j)$ is an arbitrary coupled dynamic function. We treat the system as a flow network by interpreting $f_i(t) = S(x_i) - \dot{x}_i$ as

the node-net exchanging flow at node i . The value and sign of $f_i(t)$ may change over time. If $f_i(t) > 0$, we treat node i as a source node at time t and the source flow is $f_i^s(t) = f_i(t)$. If $f_i(t) < 0$, we treat node i as a sink node at time t and the sink flow is $f_i^t(t) = -f_i(t)$. If $f_i(t) = 0$, we treat node i as a junction node at time t . Let $f_{ij}(t) = L_{ij}H(x_i, x_j)$ be the adjacent flow from node i to node j . If $f_{ij}(t) > 0$, we have $f_{ij}^{out}(t) > 0$ as the outflow from node i and $f_{ij}^{in}(t) > 0$ as the inflow at node j at time t . If $f_{ij}(t) < 0$, we have $f_{ij}^{out}(t) > 0$ as the outflow from node j and $f_{ji}^{in}(t) > 0$ as the inflow at node i at time t . By doing this interpretation, we are constructing an equivalent linear conservative flow network that instantaneously behaves in the same way as the non-linear network described by Eq. (14). This enables us to calculate the non-local interactions in the equivalent linear flow network which informs us about the non-local interactions in the original non-linear network.

We demonstrate the non-local interaction process in non-linear networks by tracing hidden flows in networks where the dynamics of nodes is described by a revised Kuramoto model [30–32], as given by

$$\dot{\theta}_i = \omega_i - K \sum_{j=1}^N L_{ij} \sin(\theta_i - \theta_j), \quad (15)$$

where K is the coupling strength, L_{ij} is the entry of the Laplacian matrix, θ_i and ω_i indicate the phase angle and natural frequency in a rotating frame, respectively. In this rotating frame, $\dot{\theta}_i = \dot{\theta}_j = 0$, $\forall i \neq j$, when the oscillators emerge into *frequency synchronisation (FS)* for a large enough K [33]. In the FS state, all the node-net exchanging flows $f_i = \omega_i - \dot{\theta}_i = \omega_i$ and all the adjacent flows $f_{ij} = KL_{ij} \sin(\theta_i - \theta_j)$ are constants, since $\sin(\theta_i - \theta_j)$ are constants.

Let $\alpha_{ij} = |f_{ij}| / \max\{|f_{ij}| : \forall i, j\}$ be a normalised variable in $[0,1]$ indicating the local interaction strength between oscillator i and j , where $\max\{|f_{ij}| : \forall i, j\}$ is the maximum of all absolute values of adjacent flows. Since $f_{ij} = -f_{ji}$, we have $\alpha_{ji} = \alpha_{ij}$. Every hidden flow is traced by considering that flows are directed. This implies that all the calculated hidden flows are non-negative and at least one of $f_{i \rightarrow j}$ and $f_{j \rightarrow i}$ is 0. We let $\beta_{ij} = \beta_{ji} = \max\{f_{i \rightarrow j}, f_{j \rightarrow i}\} / \max\{f_{i \rightarrow j} : \forall i, j\}$ be the non-local interaction strength between oscillator i and j , where $\max\{f_{i \rightarrow j}, f_{j \rightarrow i}\}$ is the non-zero one between $f_{i \rightarrow j}$ and $f_{j \rightarrow i}$, and $\max\{f_{i \rightarrow j} : \forall i, j\}$ is the maximum of all hidden flows. This definition of the non-local interaction strength allows us to compare α_{ij} and β_{ij} for the same pair of nodes in a network.

We construct three types of networks with 25 nodes, namely the Erdős-Rényi (ER) [1, 34], Watts-Strogatz (WS) [35] and Barabási-Albert (BA) models [36]. The dynamic behaviour of the nodes in these networks follows Eq. (15). The natural frequencies of oscillators are set to be random numbers in $[0,1]$. Figure 3 shows the comparison of the local interactions and the non-local interactions when the oscillators emerge into FS with a

large enough K . Figures 3 (a), (b) and (c) show the local interaction strengths, α_{ij} , for ER, WS and BA networks, respectively. Figures 3 (d), (e) and (f) demonstrate the non-local interaction strengths, β_{ij} , for ER, WS and BA networks, respectively. Figure 3 (d) exposes some hidden interactions that Fig. 3 (a) does not show to exist in an ER network. By comparing Figs. 3 (b) and (e), we see that a randomly rewired edge in a WS network not only produces interaction between the two adjacent nodes connected by this edge, but also creates functional clusters among nodes close to the two adjacent nodes. So, complex systems, such as social networks that are modelled by a WS network [37] can in fact be better connected than previously thought. We constructed the BA network by assigning smaller labels to nodes with larger degrees. Both Figs. 3 (c) and (f) illustrate the strong interactions among the nodes with large degrees (small labels). Figure 3 (c) shows that the interactions between unconnected nodes with small degrees (large labels) are weak or nonexistent, though, such interactions are revealed in Fig. 3 (f). Through this comparison, we understand that two nodes in a network may strongly interact with each other even if they are not connected by an edge.

In the supplementary material [29], we present a non-local interaction study for these networks when FS is not present. Comparing the results of the experiments with and without the existence of FS, we find that those pairs of nodes which are non-locally interacting when FS is not present also have non-local interactions in the result when FS is present. This suggests that, the existence of non-local interaction between a pair of nodes strongly depends on the network topological features of the network rather than the coupling strength.

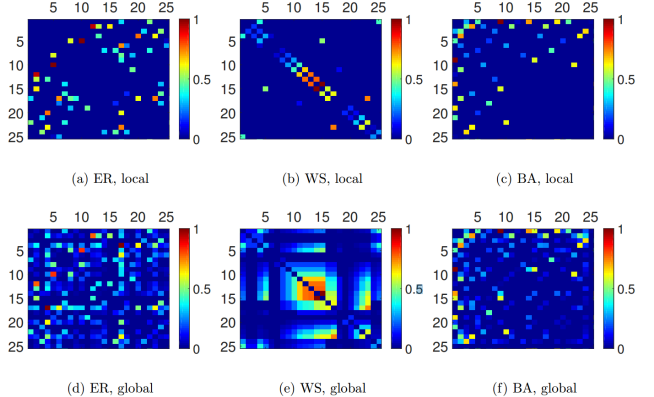


FIG. 3. (colour online) Comparison of local interactions and non-local interactions in different networks described by the Kuramoto model after the occurrence of frequency synchronisation. (a), (b) and (c) demonstrate the local interactions in ER network, WS network and BA network, respectively, compared with the non-local interactions shown in (d), (e) and (f) for these networks. The numbers on axes are labels of nodes. The colours on maps indicate the interacting strength between nodes.

Our method can also be applied to a bidirectional flow network if the network can be separated into two independent unidirectional networks. For example, under the assumption that all roads are bidirectional, we can separate the transportation network of a city into two net-

works. One network includes all the left hand roads and the other one contains all the right hand roads. Using our method, we can trace the transportation flow between any two nodes in these two networks.

[1] P. Erdos and A. Renyi, *Publ. Math. Debrecen* **6**, 290 (1959).

[2] P. Erdős and A. Rényi, *Publ. Math. Inst. Hungar. Acad. Sci* **5**, 17 (1960).

[3] D. J. Watts, *Six degrees: The science of a connected age* (WW Norton & Company, 2004).

[4] S. N. Dorogovtsev, J. F. F. Mendes, and A. N. Samukhin, *Phys. Rev. Lett.* **85**, 4633 (2000).

[5] C. Wang, N. Rubido, C. Grebogi, and M. S. Baptista, *Phys. Rev. E* **92**, 062808 (2015).

[6] C. Wang, C. Grebogi, and M. S. Baptista, *Sci. Rep.* **5**, 18091 (2015).

[7] M. Girvan and M. E. J. Newman, *Proc. Natl. Acad. Sci. USA* **99**, 7821 (2002).

[8] G. Robins, P. Pattison, Y. Kalish, and D. Lusher, *Soc. Networks* **29**, 173 (2007).

[9] K. Langendoen and N. Reijers, *Comput. Netw.* **43**, 499 (2003).

[10] A. R. Kiremire, M. R. Brust, and V. V. Phoha, *Comput. Netw.* **72**, 14 (2014).

[11] P. H. Nardelli, N. Rubido, C. Wang, M. S. Baptista, C. Pomalaza-Raez, P. Cardieri, and M. Latva-aho, *Eur. Phys. J. Spec. Top.* **223**, 2423 (2014).

[12] R. Carareto, M. S. Baptista, and C. Grebogi, *Commun. Nonlinear Sci. Numer. Simul.* **18**, 1035 (2013).

[13] W.-X. Wang, Y.-C. Lai, and C. Grebogi, *Phys. Rep.* **644**, 1 (2016).

[14] W.-X. Wang and Y.-C. Lai, *Physical Review E* **80**, 036109 (2009).

[15] D. Helbing, S. Lämmer, T. Seidel, P. Šeba, and T. Płatkowski, *Physical Review E* **70**, 066116 (2004).

[16] N. Molkenthin, K. Rehfeld, N. Marwan, and J. Kurths, *Scientific reports* **4** (2014).

[17] B. Khan, G. Agnihotri, G. Gupta, and P. Rathore, *AASRI Procedia* **7**, 94 (2014).

[18] R. Reta and A. Vargas, in *IEE Proceedings - Generation, Transmission and Distribution*, Vol. 148 (IET, 2001) pp. 518–522.

[19] D. Kirschen, R. Allan, and G. Strbac, *IEEE Trans. Power Syst.* **12**, 52 (1997).

[20] D. Kirschen and G. Strbac, *IEEE Trans. Power Syst.* **14**, 1312 (1999).

[21] J. Bialek, in *IEE Proceedings - Generation, Transmission and Distribution*, Vol. 143 (IET, 1996) pp. 313–320.

[22] Z. Jing and F. Wen, in *Transmission and Distribution Conference and Exhibition: Asia and Pacific* (IEEE, 2005) pp. 1–5.

[23] K. Xie, J. Zhou, and W. Li, *Electr. Pow. Syst. Res.* **79**, 399 (2009).

[24] M. Anuar and T. Hiyama, in *2010 Asia-Pacific Power and Energy Engineering Conference* (IEEE, 2010) pp. 1–4.

[25] A. A. Malik and N. D. Ghawghawee, *IJSER* **6**, 1124 (2015).

[26] N. P. Reddy and P. S. Raju, *IJMER* **3**, 3433 (2013).

[27] R. K. Ahuja, T. L. Magnanti, and J. B. Orlin, (1993).

[28] F. Liu, Y. Li, and G. Tang, in *2000 International Conference on Advances in Power System Control, Operation and Management.*, Vol. 1 (IET, 2000) pp. 91–95.

[29] See Supplemental Material at [URL will be inserted by publisher].

[30] Y. Kuramoto, in *International symposium on mathematical problems in theoretical physics* (Springer, 1975) pp. 420–422.

[31] Y. Kuramoto, *Chemical oscillations, turbulence and waves* (Springer, Berlin, 1984).

[32] Y. Kuramoto and I. Nishikawa, *Journal of Statistical Physics* **49**, 569 (1987).

[33] S. H. Strogatz, *Phys. D* **143**, 1 (2000).

[34] E. N. Gilbert, *Ann. Math. Stat.* **30**, 1141 (1959).

[35] D. J. Watts and S. H. Strogatz, *Nature* **393**, 440 (1998).

[36] A.-L. Barabási and R. Albert, *Science* **286**, 509 (1999).

[37] D. J. Watts, *Small worlds: the dynamics of networks between order and randomness* (Princeton university press, 1999).

Supplementary Material

I. EXAMPLE OF FLOW TRACING IN A DC NETWORK

We build up a MATLAB model to simulate a direct current (DC) network shown in Fig. 4 to illustrate the flow tracing process. The flow quantity f is given by the electric current I in this model. Nodes 1 and 2 are two nodes with current sources where $I_1^s = 3\text{A}$ and $I_2^s = 5\text{A}$, respectively. The resistances of resistors are randomly chosen within the set of integer numbers [1,10], shown in Tab. I. The sink flow leaving from the sink nodes 9 and 10 are measured by the current scopes as $I_9^t = 4.51\text{A}$ and $I_{10}^t = 3.49\text{A}$. The current directions are shown in Fig. 5. Next, we show how to calculate the source-to-sink hidden currents from the current source I_1^s and I_2^s to the sink I_9^t and I_{10}^t by different methods.

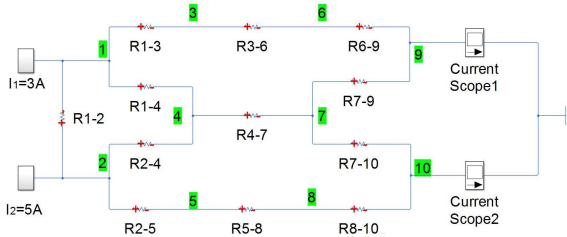


FIG. 4. The MATLAB/Simulink model for a DC network with 10 nodes.

TABLE I. Resistances of the resistors in Fig. 4.

Resistor	R_{1-2}	R_{1-3}	R_{1-4}	R_{2-4}	R_{2-5}	R_{3-6}
Resistance/ Ω	7	9	7	4	6	5
Resistor	R_{4-7}	R_{5-8}	R_{6-9}	R_{7-9}	R_{7-10}	R_{8-10}
Resistance/ Ω	1	3	2	2	3	8

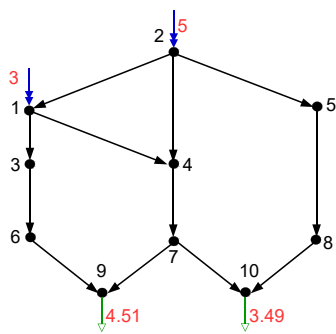


FIG. 5. The current directions in the DC network shown in Fig. 4.

A. Using the downstream Flow Tracing Method

As shown in Fig. 5, there are two paths from node 1 to node 9, which are $P_1(1, 9) = 1 \{1, 3\} 3 \{3, 6\} 6 \{6, 9\} 9$, and $P_2(1, 9) = 1 \{1, 4\} 4 \{4, 7\} 7 \{7, 9\} 9$.

Using the downstream flow tracing method, we calculate the current from node 1 to node 9 through the path $P_1(1, 9)$ by

$$I_{1 \rightarrow 9}^{(1)} = I_1^{\text{in}} \frac{I_{13}^{\text{out}}}{I_1^{\text{out}}} \frac{I_{36}^{\text{out}}}{I_3^{\text{out}}} \frac{I_{69}^{\text{out}}}{I_6^{\text{out}}} = I_1^{\text{in}} \kappa_{13}^d \kappa_{36}^d \kappa_{69}^d, \quad (16)$$

and through the path $P_2(1, 9)$ by

$$I_{1 \rightarrow 9}^{(2)} = I_1^{\text{in}} \frac{I_{14}^{\text{out}}}{I_1^{\text{out}}} \frac{I_{47}^{\text{out}}}{I_4^{\text{out}}} \frac{I_{79}^{\text{out}}}{I_7^{\text{out}}} = I_1^{\text{in}} \kappa_{14}^d \kappa_{47}^d \kappa_{79}^d. \quad (17)$$

Thus, the total node-to-node hidden current from node 1 to node 9 is

$$I_{1 \rightarrow 9} = I_{1 \rightarrow 9}^{(1)} + I_{1 \rightarrow 9}^{(2)}. \quad (18)$$

The source-to-sink hidden current is calculated by

$$I_{s1 \rightarrow t9} = \iota_1^s \cdot I_{1 \rightarrow 9} \cdot \iota_9^t. \quad (19)$$

By doing this type of calculation, we obtain $I_{s1 \rightarrow t9} = 2.35$, $I_{s1 \rightarrow t10} = 0.65$, $I_{s2 \rightarrow t9} = 2.16$ and $I_{s2 \rightarrow t10} = 2.84$.

B. Using the Upstream Flow Tracing Method

Using the upstream flow tracing method, we have

$$I_{1 \rightarrow 9}^{(1)} = I_9^{\text{out}} \frac{I_{69}^{\text{in}}}{I_9^{\text{in}}} \frac{I_{36}^{\text{in}}}{I_3^{\text{in}}} \frac{I_{13}^{\text{in}}}{I_6^{\text{in}}} = I_9^{\text{out}} \kappa_{96}^u \kappa_{63}^u \kappa_{31}^u, \quad (20)$$

and

$$I_{1 \rightarrow 9}^{(2)} = I_9^{\text{out}} \frac{I_{79}^{\text{in}}}{I_9^{\text{in}}} \frac{I_{47}^{\text{in}}}{I_7^{\text{in}}} \frac{I_{14}^{\text{in}}}{I_4^{\text{in}}} = I_9^{\text{out}} \kappa_{97}^u \kappa_{74}^u \kappa_{41}^u. \quad (21)$$

The node-to-node hidden current from node 1 to 9 is calculated by Eq. (18), and source-to-sink hidden current is calculated by Eq. (19).

Table II illustrates the results of flow tracing using the downstream flow tracing method and the upstream flow tracing method. The numbers in the following table indicate source-to-sink hidden currents. As we can see, the two methods imply the same results.

TABLE II. Flow tracing in the DC network shown in Fig. 4, where nodes 1 and 2 are source nodes, and nodes 9 and 10 are sink nodes. Numbers in the table shows source-to-sink hidden flows.

Node	Downstream		Upstream		
	9	10	9	10	
1	2.35	0.65	1	2.35	0.65
2	2.16	2.84	2	2.16	2.84

C. Using the Downstream Extended Incidence Matrix

From the MATLAB simulation results of the DC network, the downstream extended incidence matrix, \mathbf{K} , is

$$\mathbf{K} = \begin{bmatrix} 1 & -0.0378 & 0 & 0 & 0 & 0 & 0 & 0 & 0 & 0 \\ 0 & 1 & 0 & 0 & 0 & 0 & 0 & 0 & 0 & 0 \\ -0.4571 & 0 & 1 & 0 & 0 & 0 & 0 & 0 & 0 & 0 \\ -0.5429 & -0.6722 & 0 & 1 & 0 & 0 & 0 & 0 & 0 & 0 \\ 0 & -0.2900 & 0 & 0 & 1 & 0 & 0 & 0 & 0 & 0 \\ 0 & 0 & -1 & 0 & 0 & 1 & 0 & 0 & 0 & 0 \\ 0 & 0 & 0 & -1 & 0 & 0 & 1 & 0 & 0 & 0 \\ 0 & 0 & 0 & 0 & -1 & 0 & 0 & 1 & 0 & 0 \\ 0 & 0 & 0 & 0 & 0 & -1 & -0.6000 & 0 & 1 & 0 \\ 0 & 0 & 0 & 0 & 0 & 0 & -0.4000 & -1 & 0 & 1 \end{bmatrix},$$

and the downstream contribution matrix, \mathbf{C} , is

$$\mathbf{C} = \begin{bmatrix} 1 & 0.0378 & 0 & 0 & 0 & 0 & 0 & 0 & 0 & 0 \\ 0 & 1 & 0 & 0 & 0 & 0 & 0 & 0 & 0 & 0 \\ 0.4571 & 0.0173 & 1 & 0 & 0 & 0 & 0 & 0 & 0 & 0 \\ 0.5429 & 0.6927 & 0 & 1 & 0 & 0 & 0 & 0 & 0 & 0 \\ 0 & 0.2900 & 0 & 0 & 1 & 0 & 0 & 0 & 0 & 0 \\ 0.4571 & 0.0173 & 1 & 0 & 0 & 1 & 0 & 0 & 0 & 0 \\ 0.5429 & 0.6927 & 0 & 1 & 0 & 0 & 1 & 0 & 0 & 0 \\ 0 & 0.2900 & 0 & 0 & 1 & 0 & 0 & 1 & 0 & 0 \\ 0.7828 & 0.4329 & 1 & 0.6000 & 0 & 1 & 0.6000 & 0 & 1 & 0 \\ 0.2172 & 0.5671 & 0 & 0.4000 & 1 & 0 & 0.4000 & 1 & 0 & 1 \end{bmatrix}.$$

We also obtain, from the experiments, that $f_1^{in} = 3.1891$, $f_2^{in} = 5$, $\iota_1^s = 0.9407$, $\iota_2^s = 1$, $\iota_9^t = 1$ and $\iota_{10}^t = 1$. Thus, we calculate $f_{sj \rightarrow ti}$ for $j = 1, 2$ and $i = 9, 10$ by $f_{s1 \rightarrow t9} = \iota_9^t \cdot C_{91} f_1^{in} \cdot \iota_1^s = 2.35$, $f_{s2 \rightarrow t9} = \iota_9^t \cdot C_{92} f_2^{in} \cdot \iota_2^s = 2.16$, $f_{s1 \rightarrow t10} = \iota_{10}^t \cdot C_{10,1} f_1^{in} \cdot \iota_1^s = 0.65$, and $f_{s2 \rightarrow t10} = \iota_{10}^t \cdot C_{10,2} f_2^{in} \cdot \iota_2^s = 2.84$. We note that all these numbers coincide with that in Tab. II.

D. Using the Upstream Extended Incidence Matrix

Define the *upstream extended incidence matrix*, \mathbf{K}' , by

$$K'_{ij} = \begin{cases} -f_{ij}^{out}/f_j^{in} & \text{if } i \neq j, \text{ and } f_{ij} > 0, \\ 1 & \text{if } i = j, \\ 0 & \text{else.} \end{cases} \quad (22)$$

We know $f_i^{out} = \sum_{j=1}^N f_{ij}^{out} + f_i^t$, implying, $f_i^{out} - \sum_{j=1}^N f_{ij}^{out}/f_j^{in} \cdot f_j^{in} = f_i^t$. Since $f_i^{out} = f_i^{in}$, we have

$$f_i^{in} - \sum_{j=1}^N f_{ij}^{out}/f_j^{in} \cdot f_j^{in} = f_i^t. \quad (23)$$

Equations (22) and (23) imply

$$\mathbf{K}' \mathbf{F}^{in} = \mathbf{F}^t, \quad (24)$$

where $\mathbf{F}^{in} = [f_1^{in}, f_2^{in}, \dots, f_N^{in}]^T$ and $\mathbf{F}^t = [f_1^t, f_2^t, \dots, f_N^t]^T$. From $\mathbf{F}^{in} = \mathbf{K}'^{-1} \mathbf{F}^t$, we have

$$\begin{aligned} f_i^{in} &= \sum_{j=1}^N [\mathbf{K}'^{-1}]_{ij} f_j^t \\ &= \sum_{j=1}^N [\mathbf{K}'^{-1}]_{ij} f_j^{out} \cdot \iota_j^t. \end{aligned} \quad (25)$$

Let $\mathbf{C}' = \mathbf{K}'^{-1}$ be the *upstream contribution matrix* whose element, $C_{ij} = [\mathbf{K}'^{-1}]_{ij}$, is a *upstream contribution factor* indicating how much proportion of the total outflow at node j is coming from node i , i.e., $f_{i \rightarrow j} = C_{ij}' f_j^{out}$. Then, $f_{si \rightarrow tj} = \iota_i^s \cdot C_{ij}' f_j^{out} \cdot \iota_j^t$.

The upstream extended incidence matrix, \mathbf{K}' , of the DC network is

$$\mathbf{K}' = \begin{bmatrix} 1 & 0 & -1 & -0.3400 & 0 & 0 & 0 & 0 & 0 & 0 \\ -0.0593 & 1 & 0 & -0.6600 & -1 & 0 & 0 & 0 & 0 & 0 \\ 0 & 0 & 1 & 0 & 0 & -1 & 0 & 0 & 0 & 0 \\ 0 & 0 & 0 & 1 & 0 & 0 & -1 & 0 & 0 & 0 \\ 0 & 0 & 0 & 0 & 1 & 0 & 0 & -1 & 0 & 0 \\ 0 & 0 & 0 & 0 & 0 & 1 & 0 & 0 & -0.3230 & 0 \\ 0 & 0 & 0 & 0 & 0 & 0 & 1 & 0 & -0.6770 & -0.5842 \\ 0 & 0 & 0 & 0 & 0 & 0 & 0 & 1 & 0 & -0.4158 \\ 0 & 0 & 0 & 0 & 0 & 0 & 0 & 0 & 1 & 0 \\ 0 & 0 & 0 & 0 & 0 & 0 & 0 & 0 & 0 & 1 \end{bmatrix},$$

and the upstream contribution matrix, \mathbf{C}' , is

$$\mathbf{C}' = \begin{bmatrix} 1 & 0 & 1 & 0.3400 & 0 & 1 & 0.3400 & 0 & 0.5532 & 0.1986 \\ 0.0593 & 1 & 0.0593 & 0.6802 & 1 & 0.0593 & 0.6802 & 1 & 0.4796 & 0.8132 \\ 0 & 0 & 1 & 0 & 0 & 1 & 0 & 0 & 0.3230 & 0 \\ 0 & 0 & 0 & 1 & 0 & 0 & 1 & 0 & 0.6770 & 0.5842 \\ 0 & 0 & 0 & 0 & 1 & 0 & 0 & 1 & 0 & 0.4158 \\ 0 & 0 & 0 & 0 & 0 & 1 & 0 & 0 & 0.3230 & 0 \\ 0 & 0 & 0 & 0 & 0 & 0 & 1 & 0 & 0.6770 & 0.5842 \\ 0 & 0 & 0 & 0 & 0 & 0 & 0 & 1 & 0 & 0.4158 \\ 0 & 0 & 0 & 0 & 0 & 0 & 0 & 0 & 1 & 0 \\ 0 & 0 & 0 & 0 & 0 & 0 & 0 & 0 & 0 & 1 \end{bmatrix}.$$

We also obtain $f_9^{out} = 4.5132$, $f_{10}^{out} = 3.4868$, $\iota_1^s = 0.9407$, $\iota_2^s = 1$, $\iota_9^t = 1$ and $\iota_{10}^t = 1$. Then, $f_{s1 \rightarrow t9} = \iota_1^s \cdot C'_{19} f_9^{out}$, $\iota_9^t = 2.35$, $f_{s2 \rightarrow t9} = \iota_2^s \cdot C'_{29} f_9^{out} \cdot \iota_9^t = 2.16$, $f_{s1 \rightarrow t10} = \iota_1^s \cdot C'_{1,10} f_{10}^{out} \cdot \iota_{10}^t = 0.65$, and $f_{s2 \rightarrow t10} = \iota_2^s \cdot C'_{2,10} f_{10}^{out} \cdot \iota_{10}^t = 2.84$. The results are the same as that in Tab. II.

II. NON-LOCAL INTERACTIONS IN THE KURAMOTO MODEL WHEN FREQUENCY SYNCHRONISATION INEXISTENCE

Figure 6 shows the experiment results of the local interaction strength and non-local interaction strength in different types of networks, including the ER, WS and BA networks. Final results are taken by averaging the results of 100 time-points that are uniformly chosen in the time scale [10,20], i.e., $\alpha_{ij} = \sum_{k=1}^{100} \alpha_{ij}(t_k)/100$ and $\beta_{ij} = \sum_{k=1}^{100} \beta_{ij}(t_k)/100$, where $\alpha_{ij}(t_k)$ and $\beta_{ij}(t_k)$ are the values of α_{ij} and β_{ij} at the k^{th} time-point. The dynamic behaviour of the oscillators in these networks is described

by the Kuramoto model by assigning a small coupling strength, such that the oscillators are in an incoherent state.

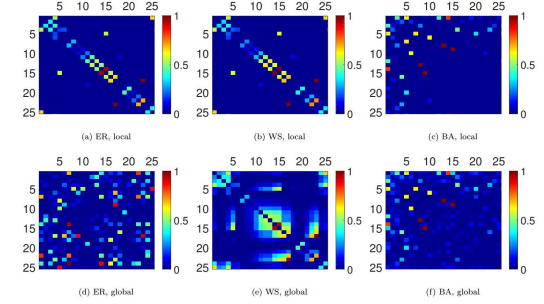


FIG. 6. Comparison of local interactions and non-local interactions in different types of networks described by the Kuramoto model when frequency synchronisation is inexistent. (a), (b) and (c) demonstrate the local interaction strength in ER network, WS network and BA network, respectively. (d), (e) and (f) show the non-local interaction strength for these networks. The numbers on axes are labels of nodes. The colour on map indicates the interacting strength between nodes.

Comparing the results in Fig. 6 with that in the paper when FS is present, we find that those pairs of nodes which are non-locally interacted when FS is not present also have non-local interactions when FS is present. This suggests that the existence of non-local interaction between a pair of nodes strongly depends on the network topological features of the network rather than the coupling strength.